

# WHAT DO WE LEARN ABOUT DENSE NUCLEAR MATTER FROM HEAVY-ION COLLISION EXPERIMENTS?\*

P. SENGER

GSI Helmholtz Institut für Ionenforschung  
Planckstr. 1, 64291 Darmstadt, Germany

*(Received January 16, 2008)*

Nucleus–nucleus collisions provide the unique opportunity to create and to investigate dense nuclear matter in the laboratory. The collision experiments address fundamental aspects of strong-interaction physics: the nuclear equation-of-state at high baryon densities, and the modification of hadron properties in the dense nuclear medium. The experimental results are relevant for our understanding of the dynamics of core-collapse supernovae, and of the structure of neutron stars. In particular, strange particles are promising diagnostic probes of dense nuclear matter. Existing experimental data, their theoretical interpretations, and future experiments will be discussed.

PACS numbers: 25.75.Dw

## 1. Introduction

Relativistic heavy-ion collisions provide a unique possibility to experimentally examine the behavior of hot and dense nuclear matter in the laboratory. The experiments offer the opportunity to study fundamental aspects of nuclear and hadron physics: the equation-of-state of baryonic matter at high densities [1], and the in-medium modifications of strongly interacting particles which might signal the onset of chiral symmetry restoration [2]. Strange mesons play a prominent role as diagnostic probes both for the properties of compressed nuclear matter and for the modifications of hadrons inside the dense medium [3, 4].  $K^+$  mesons — which contain an up and an antistrange quark — are not absorbed in nuclear matter and hence emerge from the reaction volume almost undistorted. Therefore,  $K^+$  mesons provide

---

\* Presented at the XXX Mazurian Lakes Conference on Physics, Piaski, Poland, September 2–9, 2007.

a valuable diagnostic probe for the conditions inside the dense and hot nuclear fireball. Moreover, the properties of kaons and antikaons are expected to be modified in nuclear matter.

It turned out that the sensitivity of the kaon probe to medium properties is strongly enhanced if the beam energy is below the kaon production threshold energy in nucleon–nucleon collisions. This is the case in nucleus–nucleus collision at GSI/SIS energies. Experiments on kaon and antikaon production and propagation in heavy-ion collisions at SIS have been performed with the Kaon Spectrometer (KaoS) and the FOPI detector at SIS/GSI [5–13]. In the following we review the experimental data on strangeness production which have been used to extract information on the nuclear equation of state, and on the in-medium properties of strange mesons.

## 2. The nuclear matter equation-of-state

The nuclear matter equation of state plays an important role for the dynamics of core collapse supernova and for the stability of neutron stars. In type II supernova explosions, symmetric nuclear matter is compressed to 2–3 times saturation density  $\rho_0$ . These conditions are realized in heavy-ion collisions at SIS18 beam energies, although the temperatures reached in nuclear collisions are higher than those in the core of a supernova. The study of baryonic matter at densities above  $2\text{--}3\rho_0$  has been pioneered in experiments at the AGS in Brookhaven and at the CERN-SPS, and will be one of the major research programs at the future Facility for Antiproton and Ion Research (FAIR).

The study of the equation-of-state (EOS) of (symmetric) nuclear matter is one of the most challenging goals of nuclear collision experiments. An experimental observable sensitive to the EOS is the collective flow of nucleons which is driven by the pressure built up in the reaction volume. The excitation function of the collective flow of protons has been measured in Au+Au collisions at beam energies between 1 and 8 AGeV, and the data have been analyzed with respect to the nuclear compressibility  $\kappa$  using microscopic transport calculations [1, 15]. The experimental data are shown together with the results of the transport model calculations in Fig. 1. Values of  $\kappa = 170\text{--}380$  MeV have been extracted from the data. According to the model calculations, nuclear densities between  $\rho = 2\text{--}5\rho_0$  are reached in the central fireball volume at these beam energies. Recent measurements of the collective flow of particles in Au+Au collisions at beam energies of 0.4–1.5 AGeV (corresponding to nuclear densities of about  $1\text{--}3\rho_0$ ) are compatible with values of  $\kappa = 170\text{--}230$  MeV, indicating a more soft EOS [16].

The interpretation of data using transport models is not unambiguous because the strength of the collective proton flow does not only depend on the EOS, but also on the in-medium nucleon–nucleon cross section, and

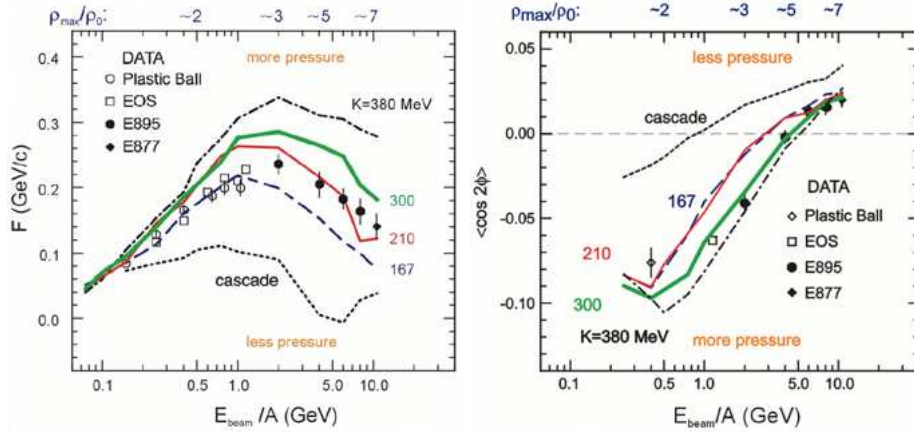


Fig. 1. Left panel: Sideward flow excitation function for Au+Au. Data and transport calculations are represented, respectively, by symbols and lines. Right panel: Elliptic flow excitation function for Au+Au. Data and transport calculations are represented, respectively, by symbols and lines (taken from [1]).

on momentum-dependent interactions. A complementary approach is to investigate the yields of newly produced particles as diagnostic probes of the nuclear compressibility. In particular, it was found that the yield of kaons created in collisions between heavy nuclei at subthreshold beam energies ( $E_{\text{beam}} = 1.58$  GeV for  $NN \rightarrow K^+ \Lambda N$ ) is sensitive to the EOS of nuclear matter at high baryon densities [3, 17, 18]. This sensitivity is due to the production mechanism of  $K^+$  mesons. At subthreshold beam energies, the production of kaons requires multiple nucleon–nucleon collisions or secondary collisions such as  $\pi N \rightarrow K^+ \Lambda$ . These processes are expected to occur predominantly at high baryon densities, and the densities reached in the fireball depend on the nuclear equation-of-state [19]. According to transport calculations, in central Au+Au collisions the bulk of  $K^+$  mesons is produced at nuclear matter densities larger than twice saturation density.

Moreover,  $K^+$  mesons are well suited to probe the properties of the dense nuclear medium because of their long mean free path. The propagation of  $K^+$  mesons in nuclear matter is characterized by the absence of absorption (as they contain an antistrange quark) and hence kaons emerge as messengers from the dense phase of the collision. In contrast, the pions created in the high density phase of the collision are likely to be reabsorbed and most of them will leave the reaction zone in the late phase.

The influence of the medium on the  $K^+$  yield is amplified by the steep excitation function of kaon production near threshold energies. Early transport calculations find that the  $K^+$  yield from Au+Au collisions at subthreshold energies will be enhanced by a factor of about 2 if a soft rather than a hard

equation-of-state is assumed [3,17,18]. Recent calculations take into account the modification of the kaon properties in the dense nuclear medium [4,20] (see next chapter). When assuming a repulsive  $K^+N$  potential as proposed by various theoretical models (see [21] and references therein) the energy needed to create a  $K^+$  meson in the nuclear medium is increased and hence the  $K^+$  yield will be reduced. Therefore, the yield of  $K^+$  mesons produced in heavy ion collisions is affected by both the nuclear compressibility and the in-medium kaon potential. The KaoS collaboration proposed to disentangle these two competing effects by studying  $K^+$  production in a very light ( $^{12}\text{C} + ^{12}\text{C}$ ) and a heavy collision system ( $^{197}\text{Au} + ^{197}\text{Au}$ ) at different beam energies near threshold [11]. The reaction volume is more than 15 times larger in Au+Au than in C+C collisions and hence the average baryonic density — achieved by the pile-up of nucleons — is significantly higher [4]. Moreover, the maximum baryonic density reached in Au+Au collisions depends on the nuclear compressibility [3,18] whereas in the small C+C system this dependence is very weak [22].

The measured excitation functions of  $K^+$  meson production in Au+Au and C+C collisions (full diamonds [11]) are depicted in the left panel of Fig. 2 together with results of QMD transport model calculations [22]. It is clearly visible that the kaon yield from C+C collision does not depend on

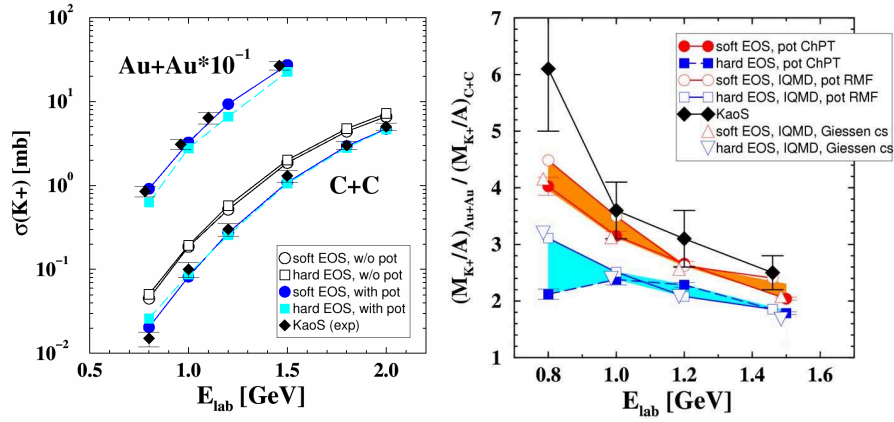


Fig. 2. Left panel: Production cross sections of  $K^+$  mesons for Au+Au and C+C collisions as a function of the projectile energy per nucleon. The data (full diamonds) are compared to results of transport calculations assuming a soft (circles) and a hard (squares) nuclear equation-of-state with and without  $K^+N$  in-medium potentials. Right panel:  $K^+$  ratio measured in inclusive Au+Au and C+C collisions as function of beam energy [11]. The data are compared to various QMD calculations assuming nuclear compressibilities of  $\kappa = 200$  MeV and 380 MeV. Taken from [14].

the nuclear EOS, but rather in the in-medium  $K^+N$  potential. Only when taking into account a repulsive kaon–nucleon potential the calculations are able to reproduce the data. The Au+Au data are in agreement with the assumption of a nuclear matter compression modulus of  $\kappa = 200$  MeV [22]. The calculations use momentum-dependent Skyrme forces to determine the binding energy per nucleon (see Fig. 3).

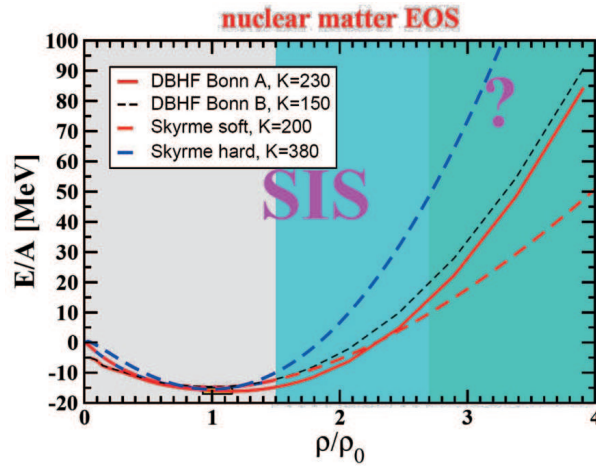


Fig. 3. Binding energy per nucleon as a function of the nuclear density obtained from relativistic Dirac–Brueckner Hartree–Fock calculations and from a phenomenological model based on Skyrme forces. Both approaches assume different values for the compressibility as indicated (taken from [14]).

In order to reduce systematic uncertainties both in experiment (normalization, efficiencies, acceptances *etc.*) and theory (elementary cross sections *etc.*) the  $K^+$  multiplicities are plotted as ratios  $(K^+/A)_{\text{Au+Au}} / (K^+/A)_{\text{C+C}}$  in the right panel of Fig. 2. In this representation also the in-medium effects cancel to a large extent. The data are compared to results of different transport model calculations [22, 23] which are performed with a compression modulus of  $\kappa = 380$  MeV (corresponding to a “hard” equation-of-state) and with  $\kappa = 200$  MeV (corresponding to a “soft” equation-of-state). The data clearly favor a soft equation of state (see right panel of Fig. 2).

Fig. 3 depicts different versions of the equation of state as predicted by different calculations [14]. The figure illustrates that it is not sufficient to determine the nuclear compressibility (which is determined by the curvature of  $E/A(\rho)$  at saturation density), but rather one has to study the response of nuclear matter at different densities, which means one has to perform nucleus–nucleus collisions at different beam energies.

### 3. In-medium properties of kaons and antikaons

According to various calculations, the properties of kaons and antikaons are modified in dense baryonic matter (see *e.g.* [4, 21, 24]). In mean-field calculations, this effect is caused by a repulsive  $K^+N$  potential and an attractive  $K^-N$  potential. As a consequence, the total energy of a kaon at rest in nuclear matter increases and the antikaon energy decreases with increasing density. As already demonstrated by the C+C data depicted in the left panel of Fig. 2 the data clearly indicate that the  $K^+N$  in-medium potential is repulsive.

The in-medium properties of  $K^-$  mesons (antikaons) are of particular interest for the stability of neutron stars. It has been speculated that an attractive  $K^-N$  potential will lead to Bose condensation of  $K^-$  mesons in the core of neutron stars above baryon densities of about 3 times saturation density [27]. In heavy-ion collisions at SIS beam energies the yield of  $K^-$  mesons should be enhanced if their effective mass is reduced in the dense medium. However, it turns out that strangeness reactions like  $\pi Y \rightarrow K^-N$  with  $Y = \Lambda, \Sigma$  also contribute significantly to the  $K^-$  yield. These multi-step processes delay the final emission (the “freeze-out”) of  $K^-$  mesons. During this delay the fireball expands and cools down, an effect which modifies the slope of the  $K^-$  spectra. The measured spectral distributions of  $K^-$  mesons exhibit a steeper slope than those of the  $K^+$  spectra. This observation is made in Ni+Ni collisions at 1.9 AGeV [13] and also in Au+Au collisions at 1.5 AGeV [12]. Due to the in-medium strangeness exchange reactions it is complicated to extract information on the  $K^-N$  potential from the measured  $K^-$  yield in heavy-ion collision. In proton–nucleus collisions — where the strangeness exchange process  $\pi Y \rightarrow K^-N$  is strongly reduced — it was found that the measured  $K^-/K^+$  ratio can be reproduced with an attractive in-medium  $K^-N$  potential of about  $-80$  MeV at saturation density [28, 29].

Another measurable consequence of in-medium  $KN$  potentials is their influence on the propagation of kaons and antikaons in heavy-ion collisions. The measured azimuthal emission patterns of  $K^+$  mesons contradict the expectations based on a long mean free path in nuclear matter. The observed sideward flow of  $K^+$  mesons [8] and the pronounced out-of-plane emission around midrapidity [6] indicate that  $K^+$  mesons are repelled from the regions of increased baryonic density as expected for a repulsive  $K^+N$  potential [25, 26].

The left panel of Fig. 4 depicts the azimuthal angle distribution of  $K^+$  mesons measured in semi-central Au+Au collisions at 1.0 AGeV [6]. The  $K^+$  emission pattern clearly is peaked at  $\phi = \pm 90^\circ$  which is perpendicular to the reaction plane. Such a behavior is known from pions which are shadowed by the spectator fragments. In the case of  $K^+$  mesons, however, the anisotropy

can be explained by transport calculations only if a repulsive in-medium  $K^+N$  potential is assumed. A flat distribution is expected when neglecting the in-medium potential [14, 30].

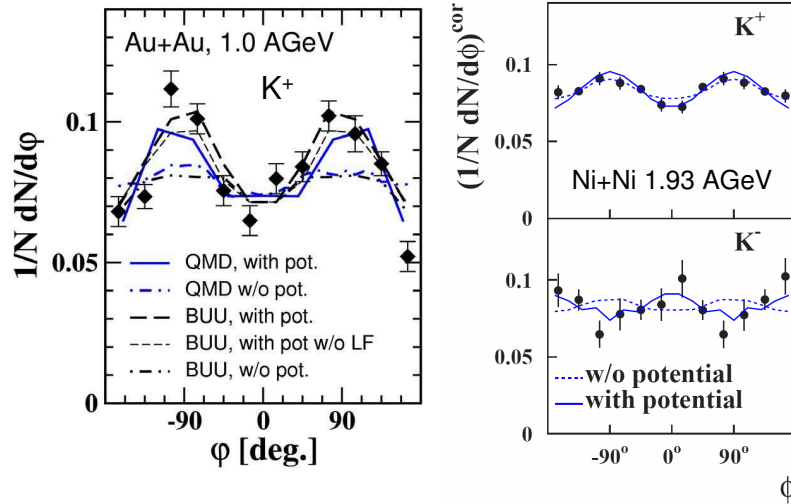


Fig. 4. Left panel:  $K^+$  azimuthal distributions for semi-central Au+Au at 1 AGeV. The data (full symbols) are compared to various transport calculations with and without in-medium potentials (see insert) [30]. Right panel:  $K^+$  and  $K^-$  azimuthal distribution for semi-central Ni+Ni collisions at 1.93 AGeV [13]. The data are corrected for the resolution of the reaction plane and refer to impact parameters of  $3.8 \text{ fm} < b < 6.5 \text{ fm}$ , rapidities of  $0.3 < y/y_{\text{beam}} < 0.7$  and momenta of  $0.2 \text{ GeV}/c < p_t < 0.8 \text{ GeV}/c$ . The lines represent results of IQMD transport calculations with and without  $KN$  potential.

The azimuthal emission pattern of  $K^-$  mesons is regarded as a key observable for the  $K^-N$  in-medium potential [26]. The existence of an attractive  $K^-N$  potential would strongly reduce the absorption of  $K^-$  mesons, and consequently the shadowing of  $K^-$  mesons by the spectator fragments would be reduced as well. In this case the  $K^-$  mesons are expected to be emitted almost isotropically in semicentral Au+Au collisions. The observation of a flat azimuthal distribution of  $K^-$  mesons would provide strong experimental evidence for in-medium modifications of antikaons. The right-lower panel of figure 4 depicts the first data on the  $K^-$  azimuthal emission pattern measured in heavy-ion collisions which differs significantly from the corresponding  $K^+$  pattern (right-upper panel) [13]. IQMD calculations including an attractive in-medium  $K^-N$  potential are able to reproduce the data [13]. Further clarification will come from high statistics data which have been measured in Au+Au collisions at 1.5 AGeV.

#### 4. What did we learn from strangeness production at SIS18?

The excitation function of  $K^+$  production measured in light and heavy collision systems at SIS energies can be reproduced by microscopic transport calculations only when assuming a soft equation of state. This result is in agreement with the interpretation of the collective flow of particles measured in Au+Au collisions. The pronounced off-plane emission (elliptic flow) of  $K^+$  mesons can be associated to a repulsive  $K^+N$  in-medium potential. The in-plane elliptic flow observed for  $K^-$  mesons can be explained with an attractive  $K^-N$  potential.

In the mean field calculations as discussed above the  $K^-$  mesons are treated as quasi-particles which are on the mass shell. Microscopic coupled-channel calculations based on a chiral Lagrangian, however, predict a dynamical broadening of the  $K^-$  meson spectral function in dense nuclear matter [31]. First off-shell transport calculations using  $K^-$  meson spectral functions have been performed [32]. The ultimate goal of the calculations is to relate the in-medium spectral function of  $K^-$  mesons to the anticipated chiral symmetry restoration at high baryon density. New experimental information on the in-medium modification of vector mesons is expected from the dilepton experiments with HADES at GSI. Highest baryon densities will be produced and explored with the Compressed Baryonic Matter (CBM) experiment at the future FAIR accelerator center in Darmstadt.

#### 5. CBM at FAIR: towards highest baryon densities

The future international Facility for Antiproton and Ion Research (FAIR) in Darmstadt will provide unique research opportunities in the fields of nuclear, hadron, atomic and plasma physics [33]. The accelerators will deliver primary beams (protons up to 90 GeV, Uranium up to 35 AGeV, nuclei with  $Z/A = 0.5$  up to 45 AGeV) and secondary beams (rare isotopes and antiprotons) with high intensity and quality. The aim of the nucleus–nucleus collision research program is to explore the QCD phase diagram at high net baryon densities and moderate temperatures. This approach is complementary to the studies of matter at high temperatures and low net baryon densities performed at RHIC and LHC. At high baryon densities, new phases of strongly interacting matter are expected. The planned Compressed Baryonic Matter (CBM) experiment is designed to explore the “terra incognita” of the QCD phase diagram at very high net baryon densities [34]. The most promising observables from nucleus–nucleus collisions in the FAIR energy range are particles containing charm quarks ( $D$ -mesons and charmonium), low-mass vector mesons decaying into dilepton pairs ( $\rho, \omega$  and  $\phi$  mesons), and hyperons ( $\Lambda, \Xi, \Omega$  and their antiparticles). This includes the measurement of (event-by-event) fluctuations, correlations, and collective flow of hadrons.

A systematic and comprehensive investigation of these observables, in particular their excitation functions, will permit to extract information on the equation-of-state of baryonic matter at high densities, on the location of the phase boundary between hadronic and partonic matter (including the QCD critical endpoint), and on the restoration of chiral symmetry at high net-baryon densities.

The experimental task is to identify hadrons and leptons in collisions with up to 1000 charged particles at event rates of up to 10 MHz. A particular experimental challenge is the identification of  $D$ -mesons which is based on the selection of secondary vertices with high accuracy. The measurements require a high-speed data acquisition (DAQ) architecture and an appropriate high-level event-selection concept.

A schematic view of the proposed CBM detector concept is shown in Fig. 5. Inside a large aperture dipole magnet there is a Silicon Tracking and Vertexing System which consists of two parts: a Micro-Vortex Detector (MVD, 2 silicon pixel layers) and the Silicon Tracking System (STS, several layers of silicon microstrip detectors). The Silicon detector array has to provide the capabilities for track reconstruction, determination of primary and secondary vertices, and momentum determination. Electrons from low-

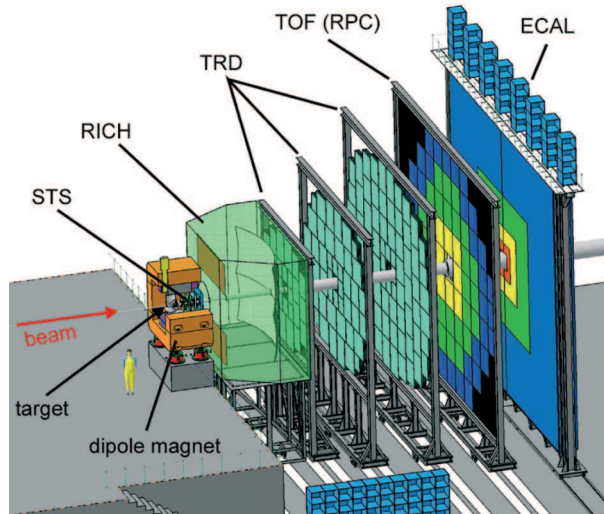


Fig. 5. Schematic view of the Compressed Baryonic Matter (CBM) experiment planned at FAIR. The setup consists of a high resolution Silicon Tracking System (STS), a Ring Imaging Cherenkov detector (RICH), three stations of Transition Radiation Detectors (TRD), a time-of-flight (TOF) system made of Resistive Plate Chambers (RPC) and an Electromagnetic Calorimeter (ECAL).

mass vector–meson decays will be identified with a Ring Imaging Cherenkov (RICH) detector. The TRD detector will provide charged particle tracking and the identification of high energy electrons and positrons. The ECAL will be used for the identification of electrons and photons. As an alternative to the RICH detector a muon detection/hadron absorber system is under investigation. If the RICH will be replaced by a muon detector the TRD will be converted into a tracking detector for hadron measurements together with the timing RPC. Then the TOF-RPC detector serves for two purposes: for background suppression during muon measurements with absorbers, and for hadron identification with muon absorbers removed.

A short illustration of the CBM physics goals, the detector layout and the expected performance is given in the “CBM flyer” [35]. Details of the feasibility studies and the detector development are presented in the CBM Progress Report 2006 [36].

I would like to thank my colleagues of the KaoS collaboration who have measured most of the data on strangeness production presented in this paper: I. Böttcher, M. Dębowski, F. Dohrmann, A. Förster, E. Grosse, P. Koczoń, B. Kohlmeyer, F. Laue, M. Menzel, L. Naumann, H. Oeschler, M. Ploskon, W. Scheinast, E. Schwab, Y. Shin, H. Ströbele, C. Sturm, G. Surówka, F. Uhlig, A. Wagner, W. Waluś.

## REFERENCES

- [1] P. Danielewicz, R. Lacey, W.G. Lynch, *Science* **298**, 1592 (2002).
- [2] C.M. Ko, V. Koch, G.Q. Li, *Annu. Rev. Nucl. Part. Sci.* **47**, 505 (1997).
- [3] J. Aichelin, *Phys. Rep.* **202**, 233 (1991).
- [4] W. Cassing, E. Bratkovskaya, *Phys. Rep.* **308**, 65 (1999).
- [5] D. Best *et al.*, *Nucl. Phys.* **A625**, 307 (1997).
- [6] Y. Shin *et al.*, *Phys. Rev. Lett.* **81**, 1576 (1998).
- [7] F. Laue, C. Sturm *et al.*, *Phys. Rev. Lett.* **82**, 1640 (1999).
- [8] P. Crochet *et al.*, *Phys. Lett.* **B486**, 6 (2000).
- [9] K. Wisniewski *et al.*, *Eur. Phys. J.* **A9**, 515 (2000).
- [10] M. Menzel *et al.*, *Phys. Lett.* **B495**, 26 (2000).
- [11] C. Sturm *et al.*, *Phys. Rev. Lett.* **86**, 39 (2001).
- [12] A. Förster *et al.*, *Phys. Rev. Lett.* **91**, 152301 (2003).
- [13] F. Uhlig *et al.*, *Phys. Rev. Lett.* **95**, 012301 (2005).
- [14] C. Fuchs, *Prog. Part. Nucl. Phys.* **56**, 1 (2006).
- [15] P. Danielewicz, [nuc1-th/0512009](https://arxiv.org/abs/nuc1-th/0512009)

- [16] A. Andronic *et al.*, *Phys. Lett.* **B612**, 173 (2005).
- [17] J. Aichelin, C.M. Ko, *Phys. Rev. Lett.* **55**, 2661 (1985).
- [18] G.Q. Li, C.M. Ko, *Phys. Lett.* **B349**, 405 (1995).
- [19] C. Fuchs *et al.*, *Phys. Rev.* **C56**, R606 (1997).
- [20] C.M. Ko, G.Q. Li, *J. Phys. G* **22**, 1673 (1996).
- [21] J. Schaffner-Bielich, J. Bondorf, I. Mishustin, *Nucl. Phys.* **A625**, 325 (1997).
- [22] C. Fuchs *et al.*, *Phys. Rev. Lett.* **86**, 1974 (2001).
- [23] Ch. Hartnack, J. Aichelin, *J. Phys. G* **28**, 1649 (2002).
- [24] G.E. Brown *et al.*, *Phys. Rev.* **C43**, 1881 (1991).
- [25] G.Q. Li, C.M. Ko, G.E. Brown, *Phys. Lett.* **B381**, 17 (1996).
- [26] Z.S. Wang *et al.*, *Eur. Phys. J.* **A5**, 275 (1999).
- [27] G.Q. Li, C.H. Lee, G.E. Brown, *Phys. Rev. Lett.* **79**, 5214 (1997).
- [28] W. Scheinast *et al.*, *Phys. Rev. Lett.* **96**, 072301 (2006).
- [29] H.W. Barz, L. Naumann, *Phys. Rev.* **C68**, 041901 (2003).
- [30] A. Larionov, U. Mosel, *Phys. Rev.* **C72**, 014901 (2005).
- [31] M.F.M. Lutz, C. Korpa, *Nucl. Phys.* **A700**, 209 (2002).
- [32] W. Cassing *et al.*, *Nucl. Phys.* **A727**, 59 (2003).
- [33] FAIR Baseline Technical Report 2006, <http://www.gsi.de/fair/reports/btr.html>
- [34] CBM Technical Status Report 2005, [http://www-linux.gsi.de/hoehne/report/cbmtsr\\_public.pdf](http://www-linux.gsi.de/hoehne/report/cbmtsr_public.pdf)
- [35] CBM Experiment, <http://www.gsi.de/documents/DOC-2007-Apr-21-1.pdf>
- [36] CBM Progress Report 2006, <http://www.gsi.de/documents/DOC-2007-Mar-137-1.pdf>